Mon. Not. R. Astron. Soc. **393,** 501–510 (2009) doi:10.1111/j.1365-2966.2008.14112.x

Absolute parameters of young stars – I. U Ophiuci

E. Budding,[1,3]★ G. İnlek[2] and O. Demircan[1]

[1]*Physics Department, University of Canakkale, TR 17020, Turkey*
[2]*Physics Department, University of Balikesir, TR 12345, Turkey*
[3]*Carter National Observatory, Wellington, New Zealand*

Accepted 2008 October 17. Received 2008 October 16; in original form 2008 July 11

ABSTRACT

We have carried out an investigation of the early-type multiple star U Oph. We have used new high-resolution spectroscopy with the High Efficiency and Resolution Canterbury University Large Echelle Spectrograph (HERCULES) and 1-m McLellan Telescope of the University of Canterbury at Mt John University Observatory and literature-sourced optical and ultraviolet photometry. We applied the local reduction package [HERCULES Reduction Software Package (HRSP)] and other software to the spectroscopic data to find radial velocities. Information limit optimization techniques (ILOT) utilizing physically realistic fitting functions were applied to these data to yield new sets of absolute parameters: $M_1 = 5.13$, $M_2 = 4.56$ (± 2 per cent); $R_1 = 3.41$, $R_2 = 3.08$ (± 1 per cent); for the early-type eclipsing binary that dominates the system. We have combined times-of-minima photometry with other data for the triple system that makes up ADS 10428A, utilizing the wide orbit of Wolf et al. as well as *HIPPARCOS* astrometry of U Oph. ILOT techniques applied to the astrometric orbit yield a mass of the third star as $0.83\,M_{\odot}$. We estimate an age of the system of around 30–40 Myr, from the isochrones of Bertelli, results given by Vaz, Andersen & Claret, as well as our own tests with an updated version of Paczyński's stellar modelling code. This age and other details are consistent with a possible origin in Gould's Belt. Such information for this, and comparable young multiple star systems, may help to clarify general properties of star formation and the subtle interactions of stars and their environment.

Key words: methods: data analysis – techniques: spectroscopic – binaries: close – stars: early-type – stars: individual: U Oph – Galaxy: stellar content.

1 INTRODUCTION

The eclipsing binary U Oph (also having the identifiers HD 156247, ADS 10428A, TYC 400-1862-1, HIP 84500, HR 6414; although not necessarily just the same thing) has been a standard reference in the evaluation of absolute parameters of early-type stars (e.g. Holmgren, Hill & Fisher 1991; Vaz, Andersen & Claret 2007). This is perhaps related to its brightness ($V = 5.903$; $B - V = 0.021$; SIMBAD), near-equator accessibility and the long historical background of awareness of its behaviour that has been discussed in many papers since the early noting of its photometric variability cycle (Gould 1879). The history of observations was given by Koch & Koegler (1977). A low light level of the binary (U Oph AB) was apparently noted by F.W. Bessel in 1823 (JD 238 6717.38), which, in principle, allows an accurate determination of the mean period over the last couple of centuries ($P = 1.677\,345\,43$ d, if we accept the reference epoch of JD 244 4416.385 65 of Wolf et al. 2002). Various early studies reported small shifts of the secondary minimum from the mid-point between primary minima, attributed to the effect of orbital eccentricity. Koch & Koegler (1977) suggested a cyclic variation on the order of 20 yr for these displacements, which could come from an apsidal motion with around that period. This question was examined in detail by Kämper (1986) and Wolf et al. (2002), who confirmed a small eccentricity ($e = 0.003$) from the analysis of times of minima. Wolf et al. found an apsidal period of 20.1 yr, fairly close to that of Kämper (1986) ($U = 20.7$ yr), as well as the value originally inferred by Koch & Koegler.

The galactic position ($\lambda = 22\overset{\circ}{.}73\,\beta = +21\overset{\circ}{.}57$), distance ($\sim$180 pc) and early type (B5Vn + B5Vn, GCVS), when taken together, suggest that the system may be associated with the Gould's Belt giant star formation region (Pöppel 1997); though this is something that invites more detailed consideration. The relevance of stars like U Oph for information on the evolution of the solar neighbourhood was also noted by Vaz et al. (2007). The main star (ADS 10428A) has a faint ($V = 12.14$) visual companion (BD + 1 3408B = ADS 10428B = U Oph D) about 20.4 arcsec to the north (Gahm, Ahlin & Lindroos 1983; Lindroos 1985). The *ROSAT* source 1RXS J171128.6+011410 is within the satellite's pointing error of ADS 10428A, but it is feasible that this source could be more directly related to ADS 10428B, to which the X-ray source's reported position is closer. The companion's magnitude and colour

★E-mail: budding@xtra.co.nz

($B - V = 0.85$), if it has a physical connection with ADS 10428A, would then make it a typical ∼G8-K0 type dwarf. Actually, Lindroos (1985; table 6) indicates that ADS 10428B shows up through an anomalous $(b - y)'$ colour, but we will find that this probably does not arise from the faint visual companion. An implication about the role of third body light also comes from the work of Ribas et al. (1998), who discussed differences between photometric and astrometric parallaxes for well-studied binaries. This matter comes up later, but we should note here that U Oph C, which does have photometric effects at longer wavelengths, is part of ADS 10428A.

Previous spectroscopic orbital parameters were determined by Plaskett (1919), Abrami (1958), Pearce (1960), Popper & Carlos (1970) and Holmgren et al. (1991). Optical light curves were produced by Huffer & Kopal (1951) and a series of ultraviolet (UV) ones given by Eaton & Ward (1973). Magalashvili (1949) also produced light curves in blue and yellow spectral regions. Koch & Koegler (1977) analysed blue and green 50 Å bandwidth scanner observations from Mt Wilson (cf. Oke 1964). They argued against a single explanation of the system's known photometric and period irregularities, and were sceptical about previous dynamical models for these.

Cester et al. (1978) analysed literature light curves using the radial velocity (RV) data of Popper & Carlos (1970). In their study, previously detected brightness and polarization variability, additional to the main binary effects, were attributed to a circumbinary gas cloud. The earlier study of Coyne (1970) is noteworthy on this point. Cester et al. considered apparent period variations in terms of a light travel time (LTT) effect, discarding the earlier suggestions of a system eccentricity. The effects of possible circumstellar matter on the spectra were taken up by Clements & Neff (1979), but they found no clear corroborative evidence. Clements & Neff used two values of the colour excess in their work however, initially considering that $E(B - V)$ could be as much as 0.25, but later preferring the more conservative 0.15, the former value being associated with an instrumental anomaly. The high colour excess would indeed suggest unusually high absorption for their distance of 275 pc, but we should note that it is difficult to resolve the observed colour of $B - V = 0.02$ with the early-type spectrum and high mass values that Clements & Neff associated with temperatures around 18 000 K. Moreover, we will find the observed V magnitude of the components to be faint with the *HIPPARCOS* (ESA 1997) distance (186 pc) even with the high colour excess, indicating something unusual about the general absorption effects towards U Oph.

This may connect with the discussions of photometric and polarimetric anomalies. Eritsian et al. (1998) concluded that there is essentially no correlation between polarization and the brightness phase of the system, although there are wavelength-dependent rapid variations. They interpreted the polarization behaviour in terms of secular wind effects (long term), punctuated by eruptive episodes (short term). Anomalous absorption effects in the line of sight seem consistent with a relatively recent star formation region in the young disc population.

Orbital period studies of the system have been carried out by various authors. Frieboes-Conde & Herczeg (1973) derived an LTT effect suggesting two possible periods of 49.3 and 55.25 yr. Panchatsaram (1981) estimated a lower value for this period, of the order of 30 yr, but urged a longer observation period for confirmation. He found the likely mass of the posited third body (U Oph C) to be around that of the Sun. A more detailed study on the times of minimum variation came from Kämper (1986), who, in addition to the previously mentioned apsidal period, confirmed the light-time effect with a period of 38.7 yr. Wolf et al. (2002), using newer times of minima, found the similar period of 37.6 yr for this wide (U Oph AB-C) orbit. Its eccentricity was found to be quite significant ($e \sim 0.2$; $\omega \sim 150^\circ$). The intermediate-period value of 38.4 yr was recently given by Vaz et al. (2007) from time of minimum analysis. Their period for the apsidal motion, 21 yr, was also somewhat closer to the earlier value of Kämper (1986) than that of Wolf et al. (2002), but all these periods (Kämper's, Wolf et al.'s and Vaz et al.'s) are within realistic probable errors of each other.

Holmgren et al. (1991) studied newer spectroscopic data, together with the photometry of Huffer & Kopal (1951) and Eaton & Ward (1973), to derive updated absolute parameters of the AB components. They found B4 and B5 spectral types. Their adopted temperatures of 16 900 and 16 000 ± 1500 K are appreciably lower than the 18 500 ± 1000 and 17 400 ± 1100 K values of Clements & Neff (1979), but they confirmed the main sequence like status of the system derived by Popper (1978) and most earlier workers. This differs from the quasi-Algol configuration adopted by Koch & Koegler (1977) using the Wilson & Devinney (1971) code. Comparison of Holmgren et al.'s parameters, found with the aid of the LIGHT fitter program that derives from Hill & Hutchings (1970), using the isochrone data of Hejlesen (1980), indicated an age of 63 Myr. This is appreciably older than the 30 Myr estimated by Kämper from the modelling of Jeffery (1986).

Vaz et al. (2007), using new *uvby* photometry with photographic coudé spectroscopy from the early 1980s taken with the 1.5-m European Southern Observatory (ESO) Telescope at La Silla, aimed to retrieve accurate absolute masses and radii for detailed comparisons with the predictions of updated stellar modelling. They found the stars in U Oph AB to have masses of 5.27 ± 0.09 and 4.74 ± 0.07 $M_\odot$, and radii of 3.48 ± 0.02 and 3.11 ± 0.03 $R_\odot$. They compared these values with several other similar early-type eclipsing binaries and were able to locate them all in a main-sequence band at ages of 5–100 Myr. However, uncertainties in details of the comparisons were suggestive of local variations of metallicity, implying that young disc stars form with significant local variation of metal abundance.

This article is the first of an intended series involving the Astrophysics Research Centre of the 18th March University of Çanakkale (COMU) and the Carter National Observatory of New Zealand in joint studies of properties of young southern stars, utilizing particularly Russell's (1948) and Kopal's (1959) 'Royal Road' of eclipsing binary system analysis. Observations, which started in mid-2006, have been productive with the HERCULES of the Department of Physics and Astronomy, University of Canterbury, New Zealand. This modern-technology instrument works with the 1-m McLellan Telescope at the Mt John University Observatory (∼43°59′S, 174°27′E). U Oph was one of the first stars on the list in this programme. In the following section, we discuss literature light curves of the eclipsing binary U Oph AB, particularly the useful series of UV light curves of Eaton & Ward (1973). The results are then combined with the analysis of our new spectroscopic material in Section 3 to refine the knowledge of the absolute parameters of the components, concentrated on in Section 4. Alternative techniques are employed for the spectroscopic reductions, including IRAF-based methods together with line-profile fitting. Rotational velocity determinations of the U Oph AB components and comparisons with stars listed in Slettebak et al. (1975) are given in Section 3.2. Most of the paper, in fact, is focused on these two massive early-type stars.

In Section 5, we consider available times of minimum data, including some historic gamma-velocities and our present results. These findings are combined with *HIPPARCOS* intermediate astrometric measurements to provide a likely mass of the third body. We

Table 1. Photometric curve-fitting results for U Oph using the ILOT curve-fitting procedure.

Parameter	Value	Error (sd)
T_h (K)	15 500	
T_c (K)	14 700	
q	0.92	
L_1-138	0.626	0.016
L_1-155	0.620	0.011
L_1-192	0.621	0.0079
L_1-246	0.612	0.0066
L_1-298	0.597	0.0090
L_1-333	0.593	0.0061
L_1-425	0.572	0.0095
L_1-Hip	0.564	0.012
L_1-Kop	0.561	0.010
r_h (mean)	0.270	0.003
r_c (mean)	0.244	0.003
i (°)	88.2	0.3
e	0.003	
ω(°) (1970.3)	345	30

*There are about 90 points, typically, in the seven UV light curves, with the quality deteriorating, slightly, towards the very short wavelengths. The temperature ratio of about 1.056 is confirmed by the trend of the luminosity ratio L_1/L_2.

consider the evolutionary stage of the binary and age determinations in Section 6, seeking also to relate our findings to properties of the Gould's Belt star-forming environment.

2 PHOTOMETRIC ANALYSIS

We examined the seven UV light curves of U Oph obtained with the OAO2 satellite, given by Eaton & Ward (1973). These are generally good-quality data sets that should yield reliable parameters for both stars. An ILOT technique[1] with an updated photometric fitting function, allowing for different density distribution options, has been used for this (Budding 2007). The results are listed, with formal errors for optimized parameters, in Table 1 (using standard symbols), and a corresponding set of corresponding curve fits shown in Fig. 1.

With the fractional luminosities of Table 1, the primary's V magnitude becomes $5.903 + 0.618 = 6.521$. Using the *HIPPARCOS* distance of 186 pc and an apparent $B - V$ colour excess of 0.19, a typical value of the ratio $R_V = A_V/E_{B-V} = 3.3$ gives the absolute magnitude as $M_V = -0.46$. This is significantly fainter than typical main-sequence stars of around B5 spectral type. There could be several explanations for this, relating to the type classification being too early for the observed colour, that is an anomalous local absorption effect. MOreover, the star may be younger than typical B5 dwarfs of the galactic field (Section 6).

Table 1 also lists fittings to the *HIPPARCOS* light curve and that of Huffer & Kopal (1951). Free fittings for the two V fractional luminosities gave rise to better overall fits with the inclusion of a slight amount of third light (average $L_3 = 0.009$). This would be with the expected level of photometric contribution of a third star about 4.6 (+0.2, −1.0) mag fainter than the main components, but cannot be considered very significant evidence in view of the scale

[1] The name 'Information Limit Optimization Technique' (ILOT) was introduced in Banks & Budding (1990). A discussion of it was given in Budding & Demircan (2007a).

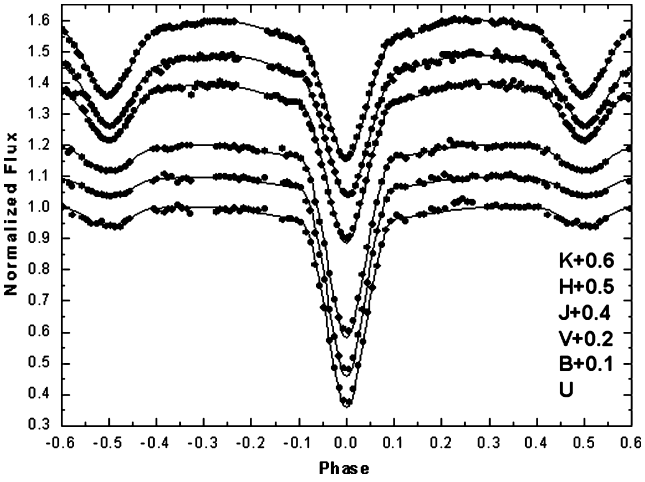

Figure 1. Light curves and fittings for the UV series of OAO2 data of Eaton & Ward (1973) on U Oph. The curves, from top to down, are in the order of increasing wavelength from 138 to 425 nm, corresponding to the fractional luminosities $L_1(\lambda)$ given in Table 1. The gradually increasing proportion of secondary light can be noticed by from the relative eclipse depths.

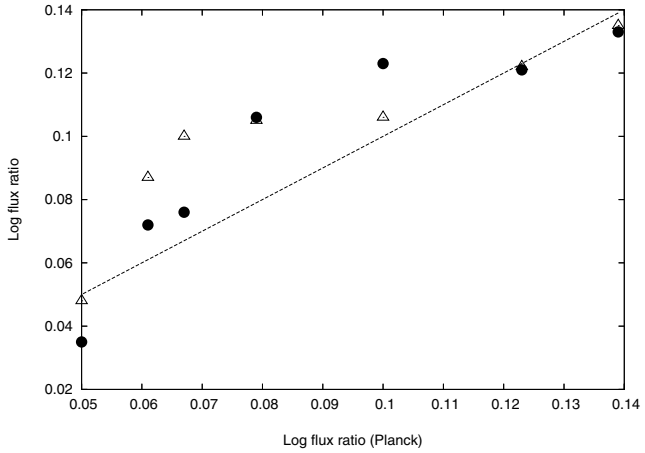

Figure 2. A check of the relative temperatures from the UV flux ratios derived from Table 1. The full line gives the logarithmic decrement ($\log F_1 - \log F_2$), at the given wavelengths, for temperatures $T_1 =$ 15 500 K and $T_2 =$ 14 700 K from the Planck formula. The Kurucz (1979) models take a more realistic account of absorption effects, and corresponding decrements for $T_1 =$ 16 000 K and $T_2 =$ 15 000 K (with $\log g = 4.0$) are shown as the full circles. The open triangles give the decrements corresponding to Table 1.

of probable errors of the determination, which are of the same order as the value itself. The parameters of Table 1 also allow a check to be made on assigned temperatures (Fig. 2). This is discussed in Section 4.

To follow up this point, photometry in the R and I bands was carried out at the Ulupinar Observatory of COMU in the spring of 2007. Curve fittings to these data, adopting the geometrical parameters from Table 1 and optimizing only for the relative luminosities, allowed R and I relative luminosities for all three components to be added to the foregoing. Utilizing the SIMBAD reference magnitudes in the J infrared region and linearly interpolating the relatively small differences in total magnitude, we then estimate the magnitudes of the three components to be as given in Table 2. The $V - R$ colour derived here is suggestive of a late G- or K-type dwarf,

Table 2. Magnitudes of stars in the U Oph (ABC) system.

	U	*B*	*V*	*R*	*I*	Err.
m_A	5.45	6.532	6.537	6.49	6.45	0.02
m_B	5.81	6.843	6.763	6.78	6.75	0.03
m_C	—	—	11.02	10.18	9.16	0.1

although the *V*-magnitude difference alone indicates a relatively brighter third star. The interpretation of this photometry may again be compromised by anomalous absorption effects, as well as the relatively large effects of measurement errors for the luminosities of the third star.

The light-curve fittings also included the effects of orbital eccentricity. Setting the value of e to that of Wolf et al. (2002), the mean anomaly at phase zero was allowed to vary. The value of ω given in Table 1 is the corresponding average for the Eaton & Ward (1973) light curves, and is in good accordance with the expected value (347°) at epoch 1970.24. The spread in individual values is considerable, however, and we do not put too much weight on the photometric derivation of this parameter for such a low eccentricity. The corresponding value obtained for the *HIPPARCOS* light curve, for example, was considerably at variance with expectation.

3 SPECTROSCOPY

The HERCULES échelle spectrograph is mounted on a stable optical bench and enclosed within a vacuum vessel located in a thermally insulated room. Light from the Cassegrain focus of the telescope is transmitted using a 20 m length of optical fibre of selectable cross-section (Hearnshaw et al. 2002). The spectrograph, at the time we collected our data, provided wavelength coverage from $\lambda = 380$ to 880 nm in over 80 orders. Image data were collected using a 4096×4096 square Fairchild back-illuminated CCD. The collecting area was subsectioned at this time, so that only part (about a third) of the full range of the orders was covered. The camera was built by Spectral Instruments, Inc., Tucson, Arizona. The pixel size is 15 μm. Two resolving powers of around $R = 35\,000$ or 70 000 are possible, enabling high precision spectroscopic observations of a variety of objects over extended times. Comparison spectra of a Thorium Argon arc lamp are recorded before and after each stellar image. Observations can be remotely controlled from inside the data room that adjoins the 1-m telescope dome, with the aid of modern image-handling software.

3.1 Line profiles

Lines identified in our observations of U Oph are listed in Table 3 together with some comment on their usefulness in subsequent analysis.

We approached the stellar absorption lines by considering first the Voigt profile, which convolves Gaussian and Lorentzian expressions, taken to reflect a kinetic distribution of radiating elements and a pressure-related damping effect. The Gaussian term dominates the central 'core' regions of the Voigt profile, while damping becomes evident in the 'wings', particularly of hydrogen. Absorption forms for real stellar lines are not simply Voigt profiles, though, as there is a well-known opacity effect that scales with $1 - \exp(-\beta)$, where β is the optical depth at a given wavelength in the profile. How to take this into account was discussed elsewhere (Budding et al. 2005), however, for lines of low central intensity there is an approximately linear proportionality of depth to number of absorbing atoms, that proves useful in the present study. For such lines, a straight convolution of Gaussian and rotational broadenings is suitable. The number of atoms contributing to a given part of the profile then varies directly with the corresponding photospheric area, Doppler shifted as appropriate. This gives rise to the relatively simple expression for the decline from continuum intensity I_c over a line of nominal depth I_d at mean wavelength λ_m:

$$I(x,\sigma,u) = I_c - \frac{3I_d}{(3-u)}\left\{(1-u)J_1(x,\sigma) + \frac{\pi}{4}uJ_2(x,\sigma)\right\}, \quad (1)$$

with

$$J_n(x,\sigma) = \int_{-\infty}^{\infty}(1-t^2)^{n/2}\exp\{-(x-t)^2/2s^2\}\mathrm{d}t \ , \quad (2)$$

where u is the limb-darkening coefficient and x is the wavelength scaled in units of the projected equatorial rotational velocity r (cf. Oláh et al. 1992). Explicit forms exist for the J_n integrals when n is even, but numerical quadrature gives fast and accurate results for any n due to the rapid convergence of the exponential term.

Table 3. Lines identified in the spectra (camera Section 2) of U Oph.

Species	Order no.	Wavelength	Comment
He I	85	6678.149	Well defined
Hα	87	6562.817	Near end of order (incomplete profile)
Si II	95	5978.97	Too weak (for reliable RV)
He I	97	5875.65	Relatively strong, but triplet status
Si II	100	5669.59	Too weak
Fe II	110	5169.030	Sometimes measurable
He I	113	5047.736	Near end of order
Hβ	117	4861.332	Strong lines, but broad and saturated
N II	119	4779.71	Too weak
He I	121	4713.201	Measurable
O II	124	4596.174	Sometimes measurable
O II	124	4590.271	Too weak
N II	125	4552.536	Too weak

3.2 Rotational velocities

Using formula (1), in an ILOT-type curve-fitting setting, we fitted selected helium line profiles of U Oph at various orbital phases. We give more procedural details in the next section. Typical results of the profile fitting are shown in Fig. 3 and Table 4.

Concerning the parameters listed in Table 4, the parameter r, that scales x in (1), measures the rotational velocity (in Å). The corresponding velocities are 104.8 and 97.8 km s^{-1} for primary and secondary, respectively. These are effectively unchanged by the inclination-related projection factor sin 88°.2. They are within the error limits of corotation, from the derived systemic rotation speed of 389 km s^{-1} and the fractional radii from Table 1, which would yield corotation values of 105 and 95 km s^{-1}, respectively. Vaz et al. (2007) calculated a synchronization time of less than 4 Myr, from which corotation would be expected, unless the system was very young.

We note that the secondary lines appear somewhat broader, in general, than the primary, and this is associated with the larger Gaussian component to the secondary lines in the fitting. This may

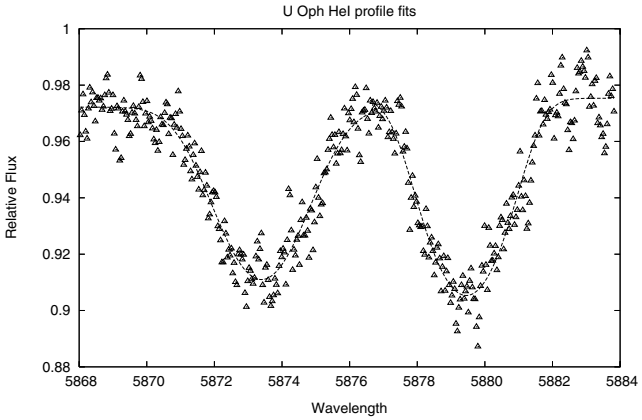

Figure 3. Results of profile fitting to the He I 5876 lines at elongation. The secondary is on the left-hand side.

Table 4. Profile fitting parameters for the He I 5875Å feature.

Parameter	Value	Error
primary		
I_c	0.975	0.005
I_d	0.059	0.007
λ_m	5879.451	0.026
r	2.053	0.032
s	0.253	0.016
χ^2/ν, Δl	1.458	0.007
Secondary		
I_c	0.972	0.005
I_d	0.052	0.008
λ_m	5873.390	0.021
r	1.915	0.029
s	0.454	0.019
χ^2/ν, Δl	1.029	0.007

be associated with the relatively greater effects of surface heating from the other star, which would give rise to considerable local turbulence (the corresponding velocity scales of $\sim$20 km s^{-1} are significantly supersonic).

3.3 Radial velocities

The mean wavelengths derived from profile fitting to the neutral helium lines allow mean (stellar) radial velocities to be derived, using the Doppler displacement principle, by comparison of these mean wavelengths with their rest values. The four He I lines listed in Table 3 were used for this purpose, with checks also being made on Hβ cores at elongation phases. Of course, this procedure should take into account other sources of apparent motion, such as the Earth's rotation and its motion around the barycentre of the solar system and Earth–Moon system. These additional corrections are found from information in the file-headers created by the HRSP (Skuljan & Wright 2007) and are applied directly. HRSP creates Flexible Image Transport Software (FITS; http://fits.gsfc.nasa.gov/) type files, which, after wavelength calibration, removal of spurious pixels (such as those struck by cosmic rays), correction for the inherent pixel-to-pixel response variation ('flat fielding') and continuum normalization, produces a string of source fluxes versus wavelength. These data can then be dealt with (if desired) by other

Table 5. Spectroscopic observations of U Oph.

No	HJD−245 0000 (d)	RV_1 (km s^{-1})		RV_2 (km s^{-1})
1	3864.0689	−15.6	aver.	
2	3868.0609	74.4		−136.7
3	3868.1067	41.7		−108.6
4	3868.1321	32.2		−78.7
5	3868.1633	33.6		−73.4
6	3870.9566	89.9		−159.3
7	3870.9984	112.4		−193.0
8	3871.0383	126.5		−205.6
9	3871.0766	135.2		−218.3
10	3871.1290	144.7		−226.8
11	3871.9922	−206.4		181.4
12	3872.0303	−203.1		175.7
13	3872.0541	−203.7		174.6
14	3872.1073	−188.6		155.8
15	3872.9359	145.7		−215.1
16	3872.9441	143.9		−209.9
17	3873.0345	109.8		−171.9
18	3873.0410	111.8		−170.9
19	3873.1228	67.3		−127.9
20	3873.9811	−55.8		42.8
21	3874.0229	−69.0		3.4
22	3874.0493	−61.7		1.7
23	3874.0857	−32.6		1.1
24	3874.0857	−23.9	aver.	
25	3874.9511	−78.3		−19.9
26	3875.0024	−90.3		47.6
27	3875.0419	−98.7		68.1
28	3875.0972	−136.7		102.5
29	3875.1587	−169.0		126.5
30	3875.2230	−194.4		147.6

software, such as that of the Image Reduction and Analysis Facility (IRAF; cf. e.g. Barnes 1993) or other procedures.

Fitting to separate (or possibly combined) model line profiles puts definite information into the RV derivation that a direct cross-correlation of the observed spectrum against a RV standard does not, particularly in relation to the location of line centres in a blended (binary) profile (see also Rucinski 2006). The direct cross-correlation option available in HRSP was tested with the early-type RV standard HR 2154 using the relevant procedure in HRSP. However, difficulties with interpreting local maxima in the cross-correlation of this spectrum with U Oph at intermediate phases in terms of genuine systemic velocities became apparent. The cross-correlation function, in principle, correlates all information in the recorded spectra – such as interpixel electron adhesion (the 'herringbone effect'), telluric lines and cloud-reflected moonlight or third body effects – that have no relation to the main binary components under study. The RVs listed in Table 5 therefore come from individual line-centre determinations, using profile model information. In the two cases of near conjunction observations, the blending is such that it is appropriate to give only single measures, presumed to be weighted averages of the combination of both spectra.

The errors of mean line centre positions in Table 4 correspond to a little over 1.0 km s^{-1} (around 0.5 per cent of their mean widths) and this is representative of individual measurement sets that led to the RV values given. However, systematic differences of this order (or greater) are also noticed between individual line shift measures. This might arise from imprecise vacuum wavelength calibration in experimental source procedures, (stellar) atmospheric, (binary)

interaction or other reasons. We believe our high resolution enables a good precision in the derived RV values, but it is important to keep in mind inherent observational limitations for these rapidly rotating, tidally distorted, interactive, early-type binary star components. So, although the RVs in Table 5 are listed to four significant digits, the last digit is optimistic.

It has been recognized for a long time that RVs in close binary systems are affected by similar kinds of proximity induced distortions are as the photometric variations. Approximations for these effects were spelled out by Kopal (1959), whose treatment of the rotational and tidal terms follows classical lines for the relevant Poisson equation. Kopal (1959) also discussed the radiative interactions between binary components, although theory, in that case, has been generally less well developed (cf. e.g. Batten 1957; Hutchings 1973; Kopal 1988). It is true, however, that in relation to errors of measurement, at least until relatively recent times, normal proximity effects introduce only small distortions to the main quasi-sinusoidal RV variation, except for very close systems. Even so, in the present computing era, there is no great difficulty to include such effects in a realistic fitting function. The situation is comparable with the RV variations through the eclipse phases, although changes to the general sinusoidal trend there (associated with the names of Schlesinger, Rossiter and McLoughlin) can become quite notable. Similarly, the effects of orbital eccentricity, even though slight in the present case, can be easily included in a general fitting function. We have introduced such a model for the RV variation for our present work, and set it in an ILOT programming environment, along similar lines to the treatment of the photometry (Budding & Demircan 2007b). Results of application of this program to the observed RVs are shown in Fig. 4.

A trial fitting with the eccentricity allowed to be a free parameter and the periastron longitude set at its expected value (103°) caused the eccentricity to increase to ∼0.03, but this result is not taken seriously concerning the orbit, in view of the other evidence [see also Kämper's (1986) comments about the spectroscopic eccentricity of Pearce (1960)]. It is sufficient to notice that systematic effects appear in the RVs that are not in the standard model. Thus, although the profile fits at elongation suggest that velocities could have errors not exceeding 1.5 km s^{-1}, actual standard deviations (if we neglect a few poorly determined measures near the conjunctions) are around

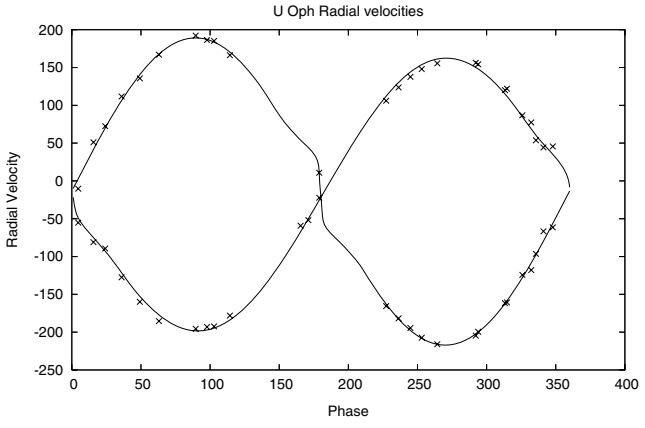

Figure 4. Measured RVs are plotted against a fitting function that takes into account both proximity and eclipse effects. The primary star approach (more negative RVs relative to the centre of mass) after phase zero. Note the Rossiter effect for the secondary around the phases of secondary eclipse (near 180°). This effect is less marked for the less eclipsed primary star (around phase 0°).

Table 6. Adopted absolute parameters for the U Oph system. Formal errors are indicated by the parenthesized numbers affecting the last retained digit of the solution (see also Section 3.3).

Parameter	Value
Period(d)	1.667 345 43
Epoch (HJD)	245 2501.1922
V_0, $(B-V)_0$, $(U-B)_0$	4.33; −0.17; − 0.03
E_{B-V}	0.19
$A_{12}(R_\odot)$	12.8(2)
$K_{1,2}$ (km s^{-1})	180.0(1.3); 202.7(1.2)
V_γ (km s^{-1})	−15.8(1.4)
$M_{1,2}(M_\odot)$	5.13(8); 4.56(7)
$R_{1,2}(R_\odot)$	3.41(3); 3.08(3)
log g (log cgs)	4.08; 4.12
V_1 (mag)	6.53
V_2 (mag)	6.80
$T_{e,1}$ (K)	17 200
$T_{e,2}$ (K)	16 200

2 km s^{-1}. Including the near conjunction measures increases the 1σ uncertainty to ∼5 km s^{-1}.

4 ABSOLUTE PARAMETERS

The fitted RVs have amplitudes that, when combined with the orbital inclination derived from the light-curve fittings, give the masses and radii presented in Table 6. These amplitudes are almost within the errors of the values given by Vaz et al. (2007), and similarly with the photometric solutions. We might then expect the absolute parameters to be closely comparable. This is almost the case for the radii, but for some reason Vaz et al. list masses that are slightly higher than their RV amplitudes would yield (by ∼0.04 $M_\odot$) if we use the latest values of the standard astronomical constants. The velocity of the centre of mass V_γ is also listed in this table. It corresponds to the region of the minimum in Kämper (1986; fig. 7), although noticeably lower than Kämper's value (∼ −13 km s^{-1}). Kämper's formula for V_γ gives a bigger amplitude when more recent parameters are inserted, even so, a small discrepancy remains.

The UV flux ratios shown in Fig. 2 confirm that there is about 1000 K difference in temperatures of the two stars, but such ratios do not allow a direct determination of individual temperatures. If we accept the independently determined masses and radii as being in fair agreement with the reported main sequence spectral types, around B5, by interpolation from table 3.6 in Budding & Demircan (2007a), the temperatures should be 17 150 and 16 150 K, respectively. This would perhaps suggest a slightly earlier spectral type than B5 for the primary (perhaps B4) and B5 for the secondary. The absolute V magnitudes turn out to be about −1.4 and −1.1 for primary and secondary, respectively. The resulting distance moduli are 2.586 for the primary, $V = 6.53$ and 2.580 for the secondary, $V = 6.80$: the average value would give a distance of 383 pc in the absence of interstellar extinction. The *HIPPARCOS* parallax requires a visual extinction of 1.57 mag. This is clearly much larger than a typical extinction going with the expected colour excess of 0.19 (Section 2). This requires the ratio $R_V = A_V/E_{B-V}$ to be ∼8. This large ratio is suggestive of a large grain population in the direction of the stars (grey extinction, cf. e.g. Draine 2003) that could be associated with the previously mentioned polarization anomalies reported by Eritsian et al. (1998).

If we use temperatures of 17 000 and 16 000 K, indicated by the foregoing discussion, for primary and secondary, we will obtain

corresponding photometric fluxes (F'_V) of 4.064 and 4.054, respectively, using the bolometric corrections from table 3.1 in Budding & Demircan (2007a). From the formula

$$\log \Pi = 7.454 - \log R - 0.2V - 2F'_V \quad (3)$$

(Budding & Demircan 2007a; equation 3.42), we derive an average photometric distance for the two stars of about 150 pc. The difference with the *HIPPARCOS* result can be resolved by reducing the adopted extinction (1.57 mag) or increasing the temperatures a little more. But in view of the uncertainties surrounding the anomalous extinction we should not put too much weight on any photometric distance in this case.

5 ASTROMETRIC AND O − C ANALYSIS, AND THIRD BODY

Bakış et al. (2006) discussed the use of *HIPPARCOS* astrometric data in the comparable case of δ Lib. In that example, the third orbit has the relatively short period of about 2.8 yr, so it would have been completed within the observation gathering period of the satellite. Although the data were relatively noisy, the nodal angle and an inclination could be estimated for the wide orbit, hence allowing an evaluation of the mass of the third star. Typical errors for *HIPPARCOS*' fixing of stellar positions are on the order of 1–2 mas. The local plane of the sky forms the reference plane and the nodal angle Ω refers the intersection line of the wide orbit in this plane to the equatorial coordinate system. Further details were given by Bakış et al. (2006).

HIPPARCOS actually records great circle abscissal measures, p, say. The variations of p in dependence on small changes of a given position of a star X_1, Y_1, Z_1, and the star's motions through the satellite's observation period, $\dot{X}_1$, $\dot{Y}_1$, $\dot{Z}_1$, for practical purposes, follow as,

$$\Delta p = \frac{\partial p}{\partial X_1}\Delta X_1 + \frac{\partial p}{\partial Y_1}\Delta Y_1 + \frac{\partial p}{\partial \Pi}\Delta \Pi_1 + \frac{\partial p}{\partial \dot{X}_1}\Delta \dot{X}_1 + \frac{\partial p}{\partial \dot{Y}_1}\Delta \dot{Y}_1 \,. \quad (4)$$

Here, Π_1 is the parallax, and ΔX_1, ΔY_1, $\Delta \dot{X}_1$ and $\Delta \dot{Y}_1$ combine the effects of systematic displacements due to an orbital motion, together with any possible constant errors in the assigned position X_1, Y_1 and proper motions $\dot{X}_1, \dot{Y}_1$ arising from neglect of such orbital effects in the original *HIPPARCOS* solution. We can then write

$$\Delta p = \frac{\partial p}{\partial X_1}(X + \delta X_1) + \frac{\partial p}{\partial Y_1}(Y + \delta Y_1) + \frac{\partial p}{\partial \Pi}\Delta \Pi_1 + \frac{\partial p}{\partial \dot{X}_1}\Delta \dot{X}_1 + \frac{\partial p}{\partial \dot{Y}_1}\Delta \dot{Y}_1 \ , \quad (5)$$

with X and Y being supplied for a given model of the orbit, in dependence on the parameters a, e, i, ω, Ω and P through standard Keplerian relations. The small constants δX_1, δY_1 (zero in the original *HIPPARCOS* solution) make up the resultant measured differences taken to be affected by orbital motion, that is $\Delta X_1 = X + \delta X_1$, $\Delta Y_1 = Y + \delta Y_1$.

To calculate where the bright binary would be at any particular time, we also need the parameter T_0 that gives the epoch of periastron passage. This is referred to the zero of the *HIPPARCOS* timing system, that is 1989.847. According to Wolf et al. (2002), from whom most of the trial astrometric parameters are taken, U Oph's wide orbit was at periastron at 1981.36 that is 7.4 yr before the zero of the *HIPPARCOS* times (the seventh parameter in Table 7).

Table 7. Astrometric curve-fitting results for the wide (third) orbit of U Oph.

Parameter	Value	Error
P (yr)	38.0	
a (mas)	10.5	
e	0.2	
ω (°)	149	
i (°)	57	3
Ω (°)	46	4
T_0 (yr)	−7.4	0.2
$\Delta\ \alpha \cos\delta$ (mas)	−1.7	0.3
$\Delta\ \delta$ (mas)	−5.0	0.2
$\Delta\ \Pi$ (mas)	0.0	
$\Delta\ \mu_\alpha$ (mas yr^{-1})	1.0	
$\Delta\ \mu_\delta$ (mas yr^{-1})	−1.4	
Error meas.	$\chi^2/\nu = 1.7$	

If, as in the case of U Oph, the period of the wide orbit is quite larger than the interval during which the satellite observations were gathered, the derived *HIPPARCOS* mean annual proper motions could be affected by the binary motion, leading to systematically different values from those averaged from terrestrial observations over very many years. For such orbits with periods ∼10 yr, measured proper motions could be non-linear over the 3–4 yr of *HIPPARCOS* data. This sometimes led the catalogue compilers to introduce extra non-linear terms (van Leeuwen & Evans 1998), though that did not happen for U Oph. But a small linear correction $\Delta \dot{X}_1$, $\Delta \dot{Y}_1$, arising from the resultant mean difference of proper motion over the *HIPPARCOS* interval, should reduce the observational scatter in a solution taking this effect into account. The Bright Star Catalogue gives the mean historic proper motions of U Oph (at 2000) as −1 and −20 mas yr^{-1} in RA and declination, respectively, whereas the corresponding *HIPPARCOS* values are −4.39 and −15.73; that is different by ∼ −3 in RA and +4 mas yr^{-1} in declination. The *HIPPARCOS* errors are here given to be around 2 mas yr^{-1}. In fact, Fig. 5 indicates that the relative drift of *HIPPARCOS* proper motions, with respect to the historic means, is in the required sense during the *HIPPARCOS* observations, but not to the extent of the differences just given. We have adopted compromise values in Table 7. These allow the points to spread out a little in the

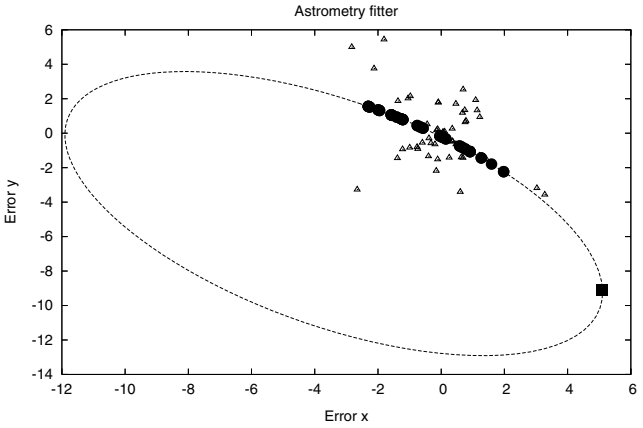

Figure 5. Fit of the wide orbit of Wolf et al. (2002) to the *HIPPARCOS* astrometry of U Oph. The triangles show the *HIPPARCOS* measures; the full circles are the corresponding orbit model predicted positions. The full square marks the position of periastron passage. The units are mas (see text).

predicted direction of motion, but larger values of μ_α and μ_δ would make this spread unacceptably large.

The five extra terms in equation (5) δX_1, δY_1, $\Delta\Pi_1$, $\Delta\dot{X}_1$ and $\Delta\dot{Y}_1$ add to the others to make up a total of 12 unknown parameters for an optimization fitting procedure. The five partial derivative coefficients are supplied as numerical tabular values for each *HIPPARCOS* position. We thus have an appropriate fitting function and corresponding data, allowing χ^2 to be calculated by a nested subroutine within an ILOT program environment. The (reduced) χ^2/ν value listed is calculated for an adopted individual *HIPPARCOS* positional error of 2 mas.

Most of the orbital parameters listed in Table 7 are adopted from Wolf et al. (2002). The inclination and nodal angle cannot be determined from time of minima analysis, however, the listed values come from optimal fitting to the *HIPPARCOS* data. Scatter is also somewhat reduced by allowing a slightly greater period than that of Wolf et al. (2002). We had adopted the value 38.0 yr from this analysis before the more recent value of 38.4 yr of Vaz et al. (2007) was published. Allowing the parallax to be a free parameter has very little effect on the solution. The adopted set of such parameters then consists of i, Ω, T_0, $\Delta\,\alpha\cos\delta$ and $\Delta\,\delta$, which are listed with corresponding error estimates. These latter two numbers locate the AB-C centre of mass with respect to the centroid of the *HIPPARCOS* measures (i.e. the origin in Fig. 5). The *HIPPARCOS* catalogue specifies such measures as 'errors' from the centroid (on the assumption of no orbital motion). The (reduced) chi-squared variate χ^2/ν was calculated with an adopted individual *HIPPARCOS* positional error of 2 mas.

The results given in Table 7 allow Kepler's law to be used to derive the mass of the third body. The value of a listed is actually $M_3/M_{12}\times A$, where A is the wide orbit's semimajor axis, since the *HIPPARCOS* observations refer only to the close binary. So, if we use solar system units, $a = 1.95$ au, and using $M_{12} = 9.69$ from Table 6 we can write:

$$a^3 = P^2 M_3^3/(M_{12}+M_3)^2 \ \text{ or}$$
$$M_3^3 = 5.135\times10^{-3}\times(9.69+M_3)^2\ . \qquad (6)$$

This yields $M_3 = 0.83$ to a satisfactory approximation. This is in keeping with the photometric findings of Section 2.

6 EVOLUTIONARY STATUS AND STELLAR ENVIRONMENT

Bertelli (2002) produced a compilation of theoretical isochrones for Gould's Belt member stars drawn from the Upper Centaurus Lupus (UCL) and Lower Centaurus Crux (LCC) regions of the Sco-Cen OB2 Association. In Fig. 6, we show the positions of the two stars of U Oph AB, according to the parameters listed in Table 6. Although it is difficult to prove a great deal from just two points, Fig. 6 corroborates both (a) that U Oph is consistent with an origin in Gould's Belt and (b) that the stars are at least as old, and probably older than most of the member stars of the Sco-Cen OB2 Association. U Oph appears older than the earliest stages of the Association, but closer to the (∼30 Myr) of Kämper (1986) than where the 63 Myr (Holmgren et al. 1991) isochrone should be expected. The latter age would correspond to the very early stages of the Gould's Belt star formation era.

U Oph is about 65° further on in longitude than the central region of the large Sco-Cen OB2 complex, which extends over ∼70° along the Belt. It has a similar proper motion in galactic latitude ($\mu_b \approx -13$ mas yr^{-1}), while there is a considerable difference in the longitude component ($\Delta\mu_l \cos b \approx 20$ mas yr^{-1}; data from above and

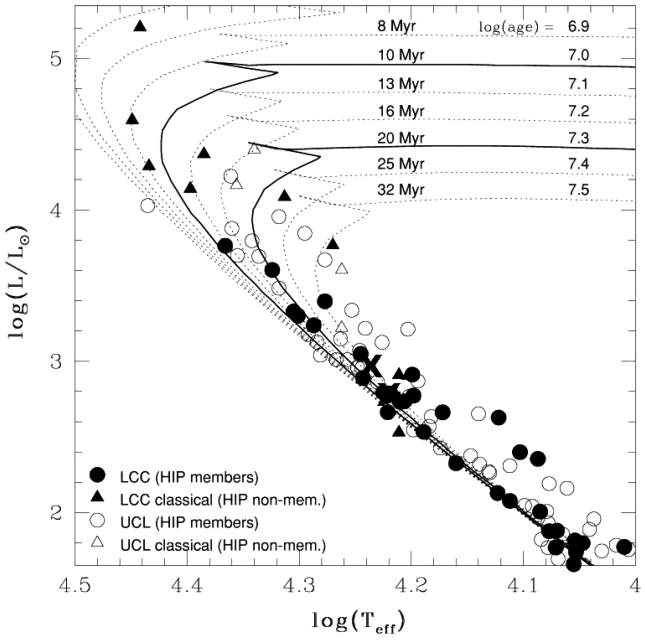

Figure 6. Theoretical isochrones of stars in the Sco-Cen OB Association according to Bertelli (2002). The positions of U Oph A and B are marked by large crosses, although the secondary is somewhat masked by crowding of the full circles.

de Zeeuw, Hoogerwerf & de Bruijne 1999) in the sense to effect the star's separation in the direction of increasing longitude. de Zeeuw, Hoogerwerf & de Bruijne (1999), in their census of the nearer OB associations, noted that the observed motions of multiple stars may be complicated by dynamical interactions between components (see also Blaauw 1988), but it is not infeasible that the system could have 'run away' from a location in Gould's Belt to the western side of the present LCC substructure.

Vaz et al. (2007) sought to test evolutionary models by reference to just the mass and radius parameters, as against colour-dependent ones. They also argued that systems with eccentric orbits have an extra possibility to check modelling via their apsidal motion constants, although the precision of that test was challenged by İnlek et al. (2008). They examined their absolute parameters for U Oph AB against a range of newer models from Claret (2004) and the Padova group (Girardi et al. 2000), which include more recent Opacity Project at Livermore (OPAL) opacities as well as possibilities for core overshooting effects and mass loss. But Vaz et al. (2007) also made cautionary remarks about this kind of comparison; for example, there are different conventions for the *exact* determination of isochrones. Moreover, the unknown free parameter of metallicity can be at least as significant in its effects as variations in the opacity tables of different source calculations (see also, İnlek et al. 2008). Yet if it could be confidently found from stellar modelling, metallicity would be an interesting parameter in Galactic contexts. Although having mass loss and overshooting parameters to play with as well as the more basic ones, Vaz et al. were still not able to match co-eval models of the same composition to both primary and secondary components of hot young binaries quite generally. If 'agreement' is stretched to mean within 1.5σ differences, then a single compromise metallicity of $Z = 0.017$ could match the four similar mass young binaries, including U Oph, that they considered. On this basis, they obtained an age of 49 Myr for U Oph AB. They

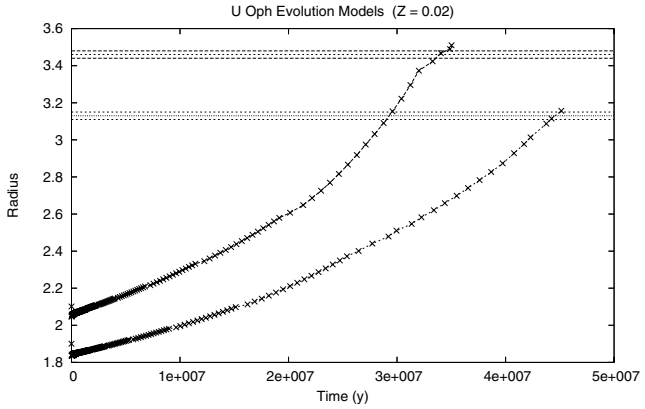

Figure 7. Evolution of the two radii of the components of U Oph according to the Paczyński (1970) code. The observed radii (with their error bounds) are shown as horizontal lines.

found a better fit for U Oph itself, however, with the slightly larger metallicity of $Z = 0.02$ and the younger age of 40 Myr.

We have used the public-domain stellar modelling codes of Paczyński (1970) to look at the structure and evolutionary status of U Oph (cf. İnlek et al. 2008). Results are shown in Fig. 7 for the same metallicity $Z = 0.02$ considered by Vaz et al. (2007). The measured radius of the primary component is attained (after an apparent shell-burning onset) at ∼33 Myr, while the secondary takes about 43 Myr. An average age of 38 Myr (close to Vaz et al.'s value) is thus found. The significant differences between the two ages seem irreconcilable with the errors of the radii, however. Tests of the Paczyński code in the vicinity of the adopted masses show considerable sensitivity of the derived radius to the zero-age model integration (the program SCH). Fig. 7 shows, for example, an initial ratio of radii of 0.895; much closer to the mass ratio (0.889) than expected for stars in this mass range, given that both the models have the same composition. While there are (at least) two parameters involved in fitting radii to evolved models, i.e. age and composition, it would normally be expected that the composition is the same for both stars (cf. e.g. Andersen 1993). A higher metallicity (e.g. $Z = 0.03$, possibly acceptable for young disc stars) brings down the average ages to around 30 Myr, close to Kämper's (1986) value. Previous observations, mentioned in the introduction, referred to local compositional anomalies. Whether the discrepancy in the ages of the two components could be explained by local anomalies or from some other effect, not considered in the simple modelling experiments performed here, remains to be settled. In view of the various uncertainties, we believe a realistic age estimate for the U Oph system is 30–40 Myr.

7 CONCLUSIONS

High resolution spectroscopy of U Oph has enabled us to derive competitively accurate radial velocities, with amplitudes similar to, but, we argue more confidently obtained than those found by other authors using lower resolution facilities. This has resulted in stellar parameters and an age of around 30–40 Myr, suggestive of a relationship to the Gould's Belt star-forming superstructure.

We have applied optimal curve-fitting techniques also to the astrometric data of the *HIPPARCOS* survey, adopting some of the parameters from Wolf et al. (2002). We then find the third star, U Oph C, to be somewhat more massive than U Oph D – the visual companion of the system. The configuration is reminiscent of Ambartsumian's (1949) scenario of the hierarchical relaxation of young multiple stars.

Future studies of young southern binaries should enable further exploration of the issues of stellar cosmogony raised in this paper.

ACKNOWLEDGMENTS

We greatly appreciate the financial support of the Turkish Science Research Council (TUBITAK) in partial support of this programme, as well as the Carter National Observatory of New Zealand. The Observatory's former Manager (J. Marchand) and former Senior Astronomer (B. Carter) provided well-received hospitality and encouragement.

Generous allocations of time on the 1-m McLennnan Telescope and HERCULES at the Mt John University Observatory were made available through its TAC and supported by its Director, Prof. J. Hearnshaw. Useful assistance at the telescope was provided by the MJUO management (A. Gilmore and P. Kilmartin) as well as (particularly) Duncan Wright and other students and staff of the Department of Physics and Astronomy, University of Canterbury, Christchurch.

V. and H. Bakış, D. Doğru and B. Özkardeş of the Department of Physics, 18th March University of Çanakkale, Turkey have given appreciated assistance with practicalities of this programme. We acknowledge also the constructive comments of Profs. M-E. Özel, A. Erdem and Z. Eker, of that department, and also Dr A. Odell of Northern Arizona University, Flagstaff, AZ., for significant help with the Paczyński code, whose testing has been assisted by O. Yılmaz and A. Böke in Çanakkale and Balikesir.

REFERENCES

Abrami A., 1958, Trieste Contrib., 3, 3
Ambartsumian V. A., 1949, Astron. Zh., 26, 1
Andersen J., 1993, in Weiss W. W., Baglin A., eds, IAU Coll. 137, Inside the Stars. Astron. Soc. Pac., San Francisco, p. 347
Bakış V., Budding E., Erdem A., Bakış H., Demircan O., Hadrava P., 2006, MNRAS, 370, 1935
Banks T., Budding E., 1990, Ap&SS, 167, 221
Barnes J., 1993, BAAS, 25, 1435
Batten A., 1957, MNRAS, 117, 521
Bertelli G., 2002, in Bienaymé O., Turon C., eds, EAS Publ. Ser. Vol. 2, GAIA: A European Space Project, p. 265
Blaauw A., 1988, Astrofizika, 29, 23
Budding E., 2007, in Demircan O., Selam S. O., Albayrak B., eds, ASP Conf. Ser. Vol. 370, ASP Conf. Ser. Vol. 40, Solar and Stellar Physics Through Eclipses. Astron. Soc. Pac., San Francisco, p. 139
Budding E., Demircan O., 2007a, An Introduction to Astronomical Photometry. Cambridge Univ. Press, Cambridge
Budding E., Demircan O., 2007b, in Gülsecen H., Limboz F., Teker A. F., eds, National Astronomy Meeting XV., Istanbul Kültür Üniv. Publ. No. 61, II. p. 969
Budding E., Bakis V., Erdem A., Demircan O., Iliev L., Iliev I., Slee O. B., 2005, Ap&SS, 296, 371
Cester B., Fedel B., Giuricin G., Mardirossian F., Mezetti M., 1978, A&AS, 33, 91
Claret A., 2004, A&A, 424, 919
Clements G. L., Neff J. S., 1979, ApJS, 41, 1
Coyne C. V., 1970, Spec. Vatic. Ric. Astron., 8, 105
de Zeeuw P. T., Hoogerwerf R., de Bruijne J. H. J., 1999, AJ, 117, 354
Draine B. T., 2003, ARA&A, 41, 241
Eaton J. A., Ward D. W., 1973, ApJ, 185, 921
Eritsian M. A., Docobo J. A., Melikian N. D., Tamazian V. S., 1998, A&A, 329, 1075

ESA, 1997, The HIPPARCOS and Tycho Catalogues, ESA SP-1200, ESA, Noordwijk
Frieboes-Conde H., Herczeg T., 1973, A&AS, 12, 1
Gahm G. F., Ahlin P., Lindroos K. P., 1983, A&AS, 51, 143
Girardi L., Bressan A., Bertelli G., Chiosi C., 2000, A&AS, 141, 371
Gould B. A., 1879, Cordoba Res., 1, 306
Hearnshaw J. B., Barnes S. I., Kershaw G. M., Frost N., Graham G., Ritchie R., Nankivell G. R., 2002, Exp. Astron., 13, 59
Hejlesen P. M., 1980, A&AS, 39, 347
Hill G., Hutchings J. B., 1970, PASP, 82, 1031
Holmgren D. E., Hill G., Fisher W., 1991, A&A, 248, 129
Huffer C. M., Kopal Z., 1951, ApJ, 114, 297
Hutchings J. B., 1973, ApJ, 180, 501
İnlek G., Böke A., Yılmaz O., Budding E., 2008, Turk J. Phys., 32, 65
Jeffery C. S., 1986, CCP7 Newsl., 10, 8
Kämper B. C., 1986, Ap&SS, 120, 16
Koch R. H., Koegler C. A., 1977, ApJ, 214, 423
Kopal Z., 1959, Close Binary Systems. Chapman & Hall, London
Kopal Z., 1988, Ap&SS, 144, 557
Kurucz R. L., 1979, ApJS, 40, 1
Lindroos K. P., 1985, A&AS, 60, 183
Magalashvili N. L., 1949, Abast. Astrofiz. Obs. Byull., 10, 1
Oláh K., Budding E., Butler C. J., Houdebine E. R., Gimenez A., Zeilik M., 1992, A&A, 259, 302
Oke J. B., 1964, ApJ, 140, 689
Paczyński B., 1970, Acta Astron., 2, 20
Panchatsaram T., 1981, Bull. Astron. Soc. India, 9, 139
Pearce J. A., 1960, AJ, 65, 55
Plaskett J. S., 1919, Publ. Dom. Astrophys. Obs., 1, 138
Popper D. M., 1978, ApJ, 220, L11
Popper D. M., Carlos R., 1970, PASP, 82, 762
Pöppel W. G. L., 1997, Fundam. Cosm. Phys., 18, 1
Ribas I., Gimenez A., Torra J., Jordi C., Oblak E., 1998, A&A, 330, 600
Rucinski S., 2006, Ap&SS, 304, 323
Russell H. N., 1948, Harvard Obs. Monogr., 7, 181
Slettebak A., Collins II G. W., Boyce P. B., White N. M., Parkinson T. D., 1975, ApJS, 29, 137
Skuljan J., Wright D., 2007, HERCULES Reduction Software Package (HRSP), version 3, Univ. Canterbury, New Zealand
van Leeuwen F., Evans D. W., 1998, A&AS, 130, 157
Vaz L. P. R., Andersen J., Claret A., 2007, A&A, 469, 285
Wilson R. E., Devinney E. J., 1971, ApJ, 166, 605
Wolf M., Harmanec P., Diethelm R., Hornoch K., Eenens P., 2002, A&A, 383, 533

This paper has been typeset from a TEX/LATEX file prepared by the author.